Available online at www.sciencedirect.com
SCIENCE DIRECT®
C. R. Chimie 8 (2005) 579–596
COMPTES RENDUS CHIMIE
http://france.elsevier.com/direct/CRAS2C/

Account / Revue

A review on the synthesis, structure and applications in separation processes of mesoporous MSU-*X* silica obtained with the two-step process

Éric Prouzet [a,*], Cédric Boissière [b]

[a] *Institut européen des membranes (CNRS UMR 5635), CNRS, 1919, route de Mende, 34293 Montpellier cedex 5, France*
[b] *Chimie de la matière condensée (CNRS UMR 7574), université Pierre-et-Marie-Curie (Paris-6) tour 54, 4, place Jussieu, 75252 Paris cedex 5, France*

Received 23 July 2004; accepted after revision 14 September 2004

Available online 18 January 2005

Abstract

We present a general review on the synthesis of mesoporous silica obtained with nonionic surfactants and bloc-copolymers as templates. This silica, referred as MSU silica, was obtained by a two-step process that led to the formation of stable hybrid micelles after a first stage of assembling between silica and surfactants, followed by the fluoride-catalyzed condensation of silica. This process allows some unique features: the final pore size can be adjusted with some synthesis parameters such as temperature or amount of catalyst, the particle shape is spherical and in the micrometric range, different shapes and nanostructures can be achieved, including hexagonal-like frameworks. Finally, we demonstrate how an accurate control of the synthesis itself may allow us to adapt this synthesis for applications dedicated to separation processes, including liquid filtration of HPLC chromatography. ***To cite this article: É. Prouzet, C. Boissière, C. R. Chimie 8 (2005).***

Résumé

Nous présentons un bilan général de la synthèse de silice mésoporeuse obtenue avec des tensioactifs non ioniques ou des copolymères tri-block. Cette silice, nommée MSU, a été obtenue par un procédé en deux étapes, qui conduit à la formation de micelles hybrides stables, après une première étape où s'effectue l'association entre oligomères de.silice et tensioactifs. Cette étape est suivie par la condensation de la silice par addition d'un sel de fluor agissant comme catalyseur. Ce procédé offre certains avantages uniques : la taille des pores peut être ajustée en jouant sur les paramètres de synthèse, tels que la température ou la quantité de catalyseur. De même, la forme et taille des particules peut être adaptée dans le domaine micronique et différentes nanostructures peuvent être obtenues avec, en particulier, des structures hexagonales en bâtonnets uniques. En conclusion, nous montrons comment l'adaptation de ce procédé de synthèse peut permettre la fabrication de matériaux spécialement dédiés à des applications séparatives telles que la filtration ou la chromatographie HPLC. ***Pour citer cet article : É. Prouzet, C. Boissière, C. R. Chimie 8 (2005).***

* Corresponding author.
E-mail address: prouzet@iemm.univ-montp2.fr (É. Prouzet).

1631-0748/$ - see front matter © 2004 Académie des sciences. Published by Elsevier SAS. All rights reserved.
doi:10.1016/j.crci.2004.09.011

Keywords: Silica; Mesoporous; Surfactant; Membrane; HPLC; Micelle

Mots clés : Silice ; Mésoporeux ; Tensioactif ; Membrane ; HPLC ; Micelle

1. Introduction

Even if the synthesis of high surface mesoporous silica had been reported in the 1970s [1], the family of mesostructured silica was actually acknowledged by the discovery of M41S materials [2,3], as well as that of mesostructured FSM-16 silica synthesized with layered silica [4,5]. These mesoporous materials were synthesized through an electrostatic interaction between cationic surfactants and silicate. A non-electrostatic way was reported shortly after by Pinnavaia's group, with the description of materials synthesized with neutral amines [6,7]. The first synthesis of mesoporous silica with the help of nonionic polyethyleneoxide (PEO)-based and block copolymers templates, in neutral pH was finally reported [8]. These latter materials were named MSU-*X* from their discovery place (*X* = 1–4 depending on the nature of the hydrophobic part of the template: alkyl, alkylaryl, block copolymer, or Tween, respectively) [8,9]. The first reactions were initially self-induced by the concentration of reagents themselves, but it was latter demonstrated that the addition of fluoride, a well-known catalyst of silica condensation, could help to the preparation of mesoporous silica prepared in pH neutral conditions [10,11]. Shortly after, the successful synthesis of SBA-15 mesoporous silica, prepared in acidic medium with copolymers was reported [12,13]. Well-ordered structures were also prepared by Su et al., with the help of nonionic surfactants [14]. In the course of our works on MSU-*X* silica, we discovered that a preparation under rather diluted concentrations and mild acidity, induced the association between silica precursors and nonionic templates, forming stable hybrid micelles. This step could be further catalyzed by the addition of a fluoride salt that led to the condensation of the silica network. This preparation defined a two-step process where the assembly step was clearly set apart from the condensation step [15–17]. This process could be employed with all kind of nonionic templates. We describe in the following the main results that we obtained during the last years. In part 2, main operations of the syntheses as well as the general structure of the mesoporous silica obtained by this approach, are described. Part 3 describes the structure of the hybrid micelles and part 4 provides examples of the different ways to change the silica nanostructure by playing with the dynamics of these hybrid micelles. In part 5, we will comment how specific morphologies are obtained and the applications regarding separation processes (membranes and HPLC) will be described in parts 6 and 7.

2. Synthesis and main characteristics

The two-step synthesis of MSU-*X* silica is based on three main factors, which makes it different from previous preparations of similar materials: concentration, pH and catalysis of silica condensation [15,16]. First, the overall concentration of nonionic PEO-based surfactants and silica source is small enough to prevent any self-induced reaction. Basically, the concentration in surfactant is close to 0.02 mol l^{-1} and the molar SiO_2:surfactant ratio lies between 8 and 12. Within this concentration range, the mixture of surfactant and silica precursors is stable for days if the reaction is proceeded in a mild acidity (pH between 1 and 4) that corresponds to a pH at which the silica precursor—usually a silicon alkoxide (TEOS: $Si(OCH_2CH_3)_4$)—is fully hydrolyzed, but not condensed, in the solution of nonionic surfactants [18]. We used mostly TEOS as a silica source even if we demonstrated that the preparation of mesoporous silica, with exactly the same characteristics, can be also achieved with sodium silicate [17]. Thirdly, the silica condensation is not induced by a pH change that leads generally to loose structures but with the addition of a fluoride salt [16].

In a typical synthesis, TEOS is added under moderate magnetic stirring in a 0.02 M solution of Tergitol 15-S-12 ($CH_3(CH_2)_{14}(EO)_{12}$, Union Carbide Chemicals) with a molar ratio TEOS:surf. = 8. TEOS is not soluble in water and the stirring must be adjusted in order to break TEOS drops in the surfactant solution. Once the mixing is complete, an unstable milky emulsion is obtained (see Fig. 1a). The addition of hydrochloric acid (final pH between 1.0 and 4.0) breaks this

emulsion within minutes, which leads to a stable colorless microemulsion (Fig. 1b). However, usually, TEOS is added directly in the acidified solution of surfactant. The solution is left at rest for 10 h and set at the desired temperature before the induction of TEOS condensation by the addition of a small amount of sodium fluoride (NaF:TEOS = 1–4 mol%). The reaction begins after a few tenth of minutes and although it is almost totally completed after 6 h, the mixture is kept for 3 days at temperature. A white powder is obtained with a yield close to 100% (Fig. 1c). It is filtered, dried and calcined at 620 °C for 6 h after a 6 h step at 200 °C (3 °C min^{-1}). This process can be carried out with the whole family of nonionic surfactants and block copolymers of MSU-*X* (*X* = 1–4) materials.

The underlying concepts of the reactions described in Fig. 2 are based on the relative hydrolysis and condensation kinetics of silica [19]. To achieve a good control on the final structure of the mesoporous silica and ease the reproducibility, both reactions (hydrolysis and condensation) must be completely separated (a complete study of the pH influence was carried out in Ref. [16]). At this dilution, between pH 1 and 4, the condensation kinetic is very low. In a surfactant-free solution, one will observe a slow gelation of a diffuse monolith after days whereas in the reacting solution containing surfactants, no reaction is observed for days.

Hence, after complete homogenization of the solution (10 h at room temperature), the silica condensation reaction can be further induced, either by a pH change or by the addition of a catalyst such as sodium fluoride or ammonium [19]. Triggering the condensation step by the addition of fluoride provides several

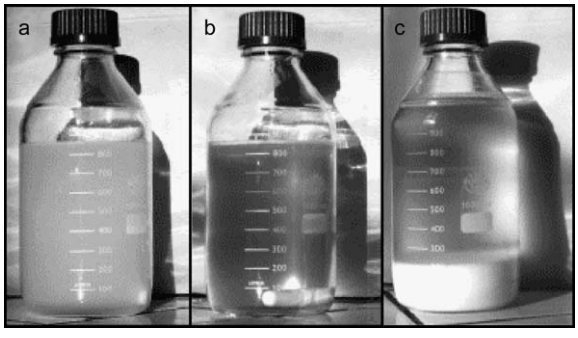

Fig. 1. Photos of the reacting medium (**a**) after addition of TEOS (mol Si:surf. = 8) in a 0.02 mol l^{-1} solution of Tergitol 15- S-12 at pH 6; (**b**) after adjustment to pH 2 and hydrolysis of TEOS; (**c**) 3 days after the addition of NaF (NaF:Si = 2% mol) and reaction at 35 °C.

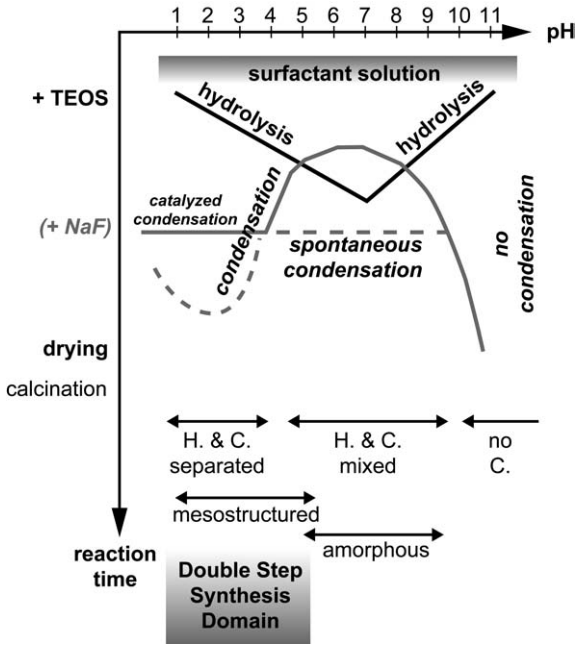

Fig. 2. Scheme of the different reaction kinetics as a function of the initial pH. For acidic pH, the TEOS hydrolysis is fast but the condensation is very low. Catalyst can be added within these two steps. For neutral pH, both mechanisms are mixed and for too basic pH, no condensation occurs at all.

advantages. The first one is that fluoride ion, as a catalyst, promotes condensation at constant pH value, avoiding the evolution of the hydroxylation rate of silica oligomers during the mesostructuration, usually met when condensation is promoted by pH evolution. This approach makes investigation of inorganic–organic interaction mechanisms simpler and final structure highly reproducible. The second one is that the condensation reaction remains localized on the silica seeds created by the catalyst. The final product is then obtained by the continuous growth of these seeds, fed by the homogeneous medium around them. This explains why rather monodisperse spherical particles are usually obtained by this process. Moreover, this provides a way to control the reaction, not only with time but also in space if fluoride catalyst is added in a specific area of the reactor. This latter property was used for the formation of supported membranes.

One of the advantages of this synthesis lies in its process at ambient pressure and at moderate or at room temperature (the reaction yield is close to 100%). It does not require any autoclave and the scaling up remains easy because the intermediary step gives a homoge-

neous and stable mixture, whatever its volume. Since the second step is induced by the addition of a solution of sodium fluoride, the homogenization is rapid and the silica condensation begins in a homogeneous mixture too. Moreover, we determined that a large amount (between 30% and 75%) of surfactant involved in the synthesis is further expelled into the mother liquor and can be easily recovered once the silica network is formed. Besides the fact that nonionic surfactants are cheap, non-toxic and biodegradable, this point decreases the overall cost and environment impact of this synthesis process.

Both hydrothermal and pressure resistance of this new material were also controlled with syntheses using sodium silicate as silica source. We demonstrated that the porous structure was preserved, even after the application of a constant pressure (600 bar) for 3 h. Powders left for 24 h in water, either at room temperature or in boiling water, suffered only of a slow hydrolysis [17]. Therefore these results let us think that an additional operation proceeded in the synthesis pathway, such as that based on seed-induction reported by Pinnavaia's group, would lead to steam-resistant materials [20]. One of the main features of silica powders obtained by this method is the spherical shape of the particles in the micrometric range (Fig. 3). This shape is the result of the nucleation and growth mechanism induced by the formation of silica seeds created by fluoride ions and followed by the isotropic aggregation of the precursors around these seeds.

This mechanism leads to a narrow particle size distribution in the 1–10 μm range (Fig. 4). The X-ray diffraction pattern exhibits a single peak characteristic of a 3D wormhole structure (Fig. 5).

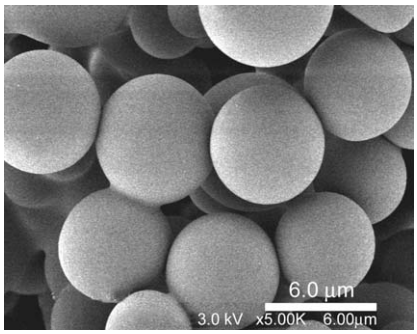

Fig. 3. SEM observation of calcined MSU silica synthesized at 35 °C with Tergitol 15-S-12, after a preliminary structuration step at pH 2 and a silica condensation induced by the addition of a NaF:TEOS molar ratio of 4%. All particles exhibit a spherical shape with some grain boundaries.

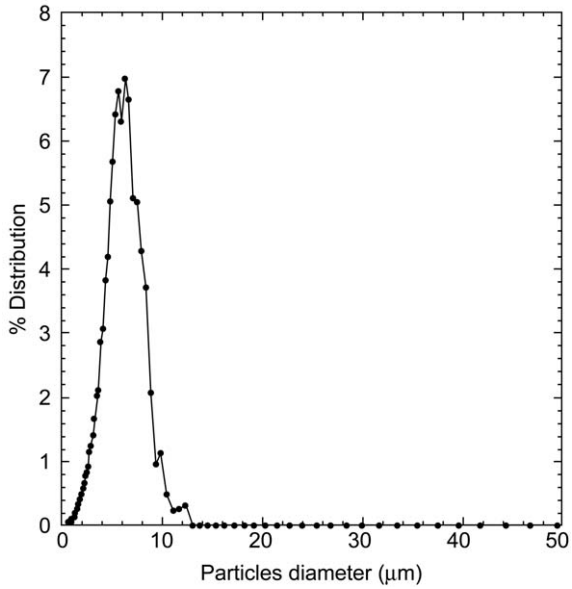

Fig. 4. Volume-averaged particle size distribution of the silica synthesized at 35 °C with Tergitol 15-S-12, after a preliminary structuration step at pH 2 and a silica condensation induced by the addition of a NaF:TEOS ratio of 4 mol%. The general particle size is defined in a 1–10 μm range.

It was the first time that such a structure was reported for a mesostructured silica [8]. We assigned this diffraction pattern to a unique correlation length in the material that could be ascribed to the pore center to pore center distance [11]. However, it is worth to point out that this structure would be better described by the disordered open connected (DOC) model that explains why a structure without long-range order, can still exhibit a single diffraction peak [21,22]. Finally, the pore structure obtained by nitrogen adsorption/desorption isotherms, shows that these materials do not exhibit any textural porosity, a clue of the homogeneous internal structure of these particles (Fig. 6). Their mean surface area ranges generally between 700 and 1000 $m^2\ g^{-1}$ (a full set of physico-chemical properties obtained with different surfactants can be found in [16,23]).

3. Structure of the intermediates

One question arose from this synthesis pathway: if the silicon alcoxide is hydrolyzed in mild acidity, in

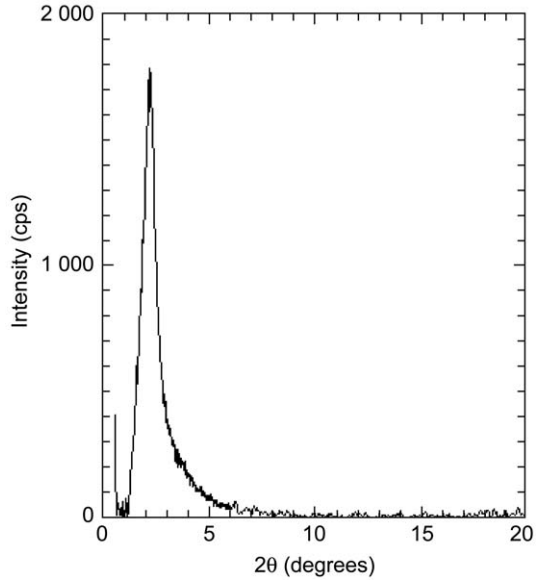

Fig. 5. XRD pattern of calcined MSU-1 silica obtained with Tergitol 15-S-12 and a NaF:TEOS ratio of 4 mol% (background extracted). The XRD pattern exhibits a single peak characteristic of a single correlation length in the material.

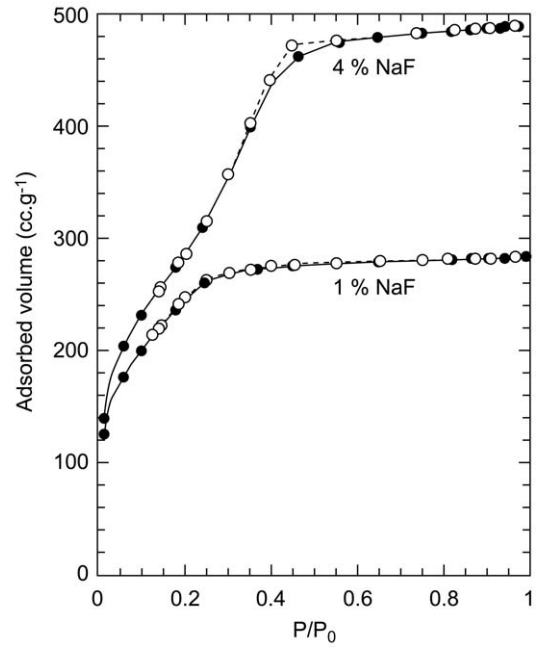

Fig. 6. Nitrogen adsorption (black dots) and desorption (white dots) isotherms of MSU-1 silica synthesized with Tergitol 15-S-12 and different NaF:TEOS molar ratios. The shift in the adsorption step reveals an increasing pore size as the amount of catalyst increases.

the presence of surfactants, do these precursors remain solubilized in water or do they associate with the surfactants? Assuming that the last point was confirmed, what would be the structure of the resulting objects? We answered these questions by demonstrating that silica oligomers obtained by the hydrolysis of TEOS are short, poorly reticulated and that they associate actually with surfactant molecules to form hybrid micelles that are stable for weeks [24]. The structure solving of these objects was obtained from apparently contradictory results obtained from small angle X-ray scattering (SAXS) and dynamic light scattering (DLS). We studied solutions with TEOS hydrolyzed at pH 2, in the presence of Tergitol 15-S-12, with TEOS:surf. molar ratios varying from 4 to 24. All solutions were totally transparent and stable before measurements. First, it was demonstrated by SAXS that TEOS dissolved and hydrolyzed in a surfactant-free solution at pH 2, does not give any scattering object. This means that the silica oligomers obtained by the hydrolysis of TEOS are very small and at the molecular level. Secondly, we studied the evolution of this solution with time and we confirmed that the pristine silica oligomers form progressively a monolithic gel with a very opened structure (Porod slope of –1.9) [24]. ^{29}Si liquid NMR confirmed the low reticulation with 50% of Q^2 (two connecting Si–O–Si bonds) and Q^3 (three connecting Si–O–Si bonds) entities.

This behavior is not observed when TEOS is hydrolyzed in a solution of Tergitol 15-S-12 (0.02 M). Actually, the SAXS patterns of these solutions (4 < TEOS:surf. < 24) exhibit only slight modifications, whatever the TEOS:surf. ratio (Fig. 7). A common minimum observed at ca. Q = 0.09 Å^{-1}, corresponds to a characteristic length of spherical objects varying from ca. 6.6 to 7.3 nm for Si/surf. ratios of 0 and 4, respectively. This distance is consistent with the diameter of a pure micelle. Positions of these minima, remain constant and equal to 0.085 Å^{-1} for higher ratios. Its intensity is the highest for Si/surf. ratios of 2 and 4, and it decreases and becomes rather constant for higher ratios. One might conclude from the SAXS experiments that the increasing amount of silica oligomers does not modify drastically the pristine micelles and that there are no specific interaction between silica oligomers and surfactants. However, this first explanation was totally in contradiction with the DLS results.

Two representative correlation functions of the TEOS:surf. = 0 and the TEOS:surf. = 23 samples cal-

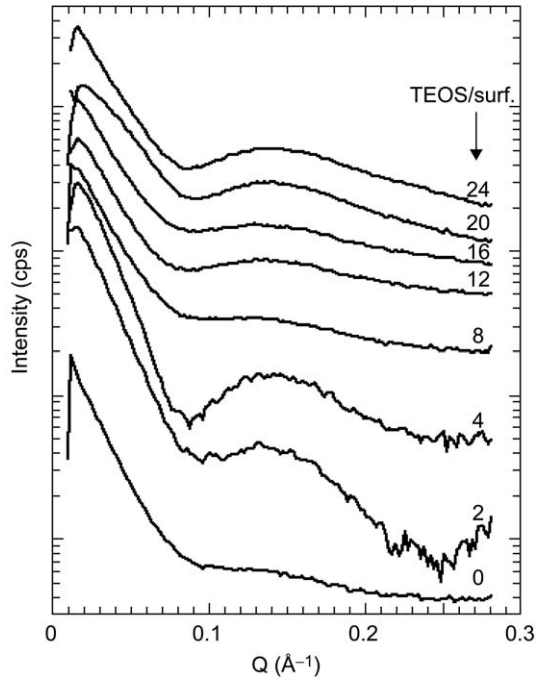

Fig. 7. Evolution of the X-ray small angle scattering of solutions prepared with different Si:surf. molar ratios. As Si:surf. increases, one observes a common curve shape.

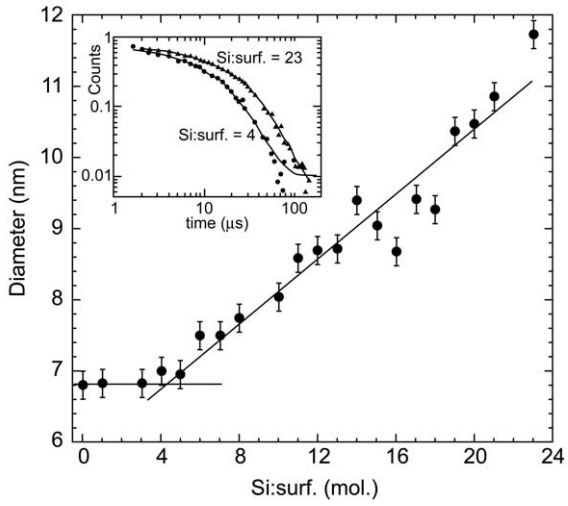

Fig. 8. Evolution of the apparent hydrodynamic diameter from DLS of the micellar hybrid objects as a function of the Si:Tergitol 15-S-12 molar ratio. All objects are spherical and monodisperse. If there is a plateau for the lowest ratios, the diameter increases linearly up to very high values and one manages to stabilize spherical objects up to 11 nm in diameter.

culated from DLS are displayed in the inset of Fig. 8, along with their single-exponential fit, which confirms the perfect agreement of the correlation function with a monodisperse size distribution for the whole range of size (all the correlation function curves were fitted with a good agreement by using a similar single-exponential fit).

Fig. 8 displays the evolution of the diameters deduced from these fits, as a function of the molar TEOS:surf. ratio. Pure Tergitol 15-S-12 micelles exhibit a mean hydrodynamic diameter of 6.8 nm, which remains constant up to a Si:surf. molar ratio of 4. For higher ratios, one observes a linear size increase up to ca. 12 nm.

Hence, it appears that DLS detects drastic changes in the micellar size, which were not detected by SAXS. We explained these apparent contradictions by going back to the physical origin of these two techniques. DLS probes the motion of objects through the measurement of the diffusion coefficient, which is related to the apparent hydrodynamic radius by the Stokes–Einstein relation. SAXS probes the electron density contrast in the medium, which can be related with correlation dimensions, such as the object size, by the scattering curve. Even if these techniques are able to bring information on the objects dimensions, they do not derive from the same physical properties, which is likely the source of this apparent contradiction. In this study, SAXS and DLS are not opposite but complementary. The structural evolution (see [24] for a complete analysis) can be summarized as reported in Fig. 9.

As the TEOS:surf. ratio increases, they evolve from pure micelles (TEOS:surf. = 0) to hybrid micelles where small silica oligomers polymerize in the palisade layer (Si:surf. = 4). It is worth to point out that our first analyses by DLS revealed a similar behavior but it was misinterpreted [8]. As the Si:surf. ratio increases above 4, these lowly reticulated oligomers extend out of the palisade layer, but the polymerization reaction still occurs, leading to the size increasing detected by DLS. However, as SAXS is a technique sensitive to the electron density contrast, the silica network concentration is too low (it was estimated to a Si:H_2O molar ratio of 1:30) to modify significantly the SAXS pattern, which explains why SAXS detects only the electron contrast created by the pristine micellar object. Several hypotheses explain why silica polymerizes at pH 2–4, in the PEO shell, but not in bulk water. Terminal OH groups

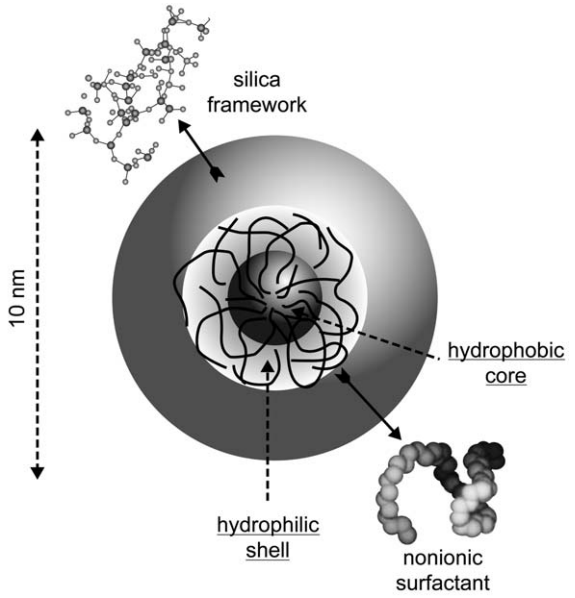

Fig. 9. Scheme of the hybrid micelle shape, as probed by DLS and SAXS. It is built from the initial micelle with the hydrophobic core made of the surfactant alkyl tails, a surrounding hydrophilic palisade formed by the PEO chains and a silica outer shell, starting in the PEO shell and growing outside when the Si:surf. ratio increases.

of the PEO chains are more nucleophilic than water and interactions between bound water molecules acting as general bases and EO groups, make them better nucleophiles than bulk water molecules. In addition, the relative local concentration of silica oligomers confined in the PEO shells is considerably higher than that in bulk water. Moreover, the local arrangement of molecules in this shell reduces the entropic loss in polymerization and therefore assists reaction.

These hybrid micelles are not only curiosities observed in the course of a synthesis, but they offer also new opportunities in the field of mesostructured materials. Indeed, they exhibit the same general behavior as usual nonionic micelles, with by example, a reversible size variation as a function of temperature. Besides, if they cannot be prepared for concentrations below the surfactant critical micelle concentration (cmc), they can be diluted afterwards and still stay stable below the cmc, preserved by the silica shell. On the reverse, if one cannot prepare directly a concentrated solution because the self-condensation of silica prevents it, the initial solution of hybrid micelles can be concentrated up to 80–90% without any reaction. In our previous studies, we claimed that these hybrid micelles, which form very stable objects, represented promising building units in further syntheses. Recent works presently under progress confirm this first assumption and these hybrid micelles must be seen as actual secondary building blocks for the preparation of nano- or meso-structured compounds.

4. The nanostructure control

One of the main goals of researchers in the field of mesostructured silica was the possibility to easily adapt the final pore size. Usually, the addition of swelling agents such as 1,3,5-trimethyl benzene (TMB) or the change in length of the surfactant hydrophobic chain were the main parameters that helped to control the final pore size in these mesostructured materials. Same behavior was also observed with the MSU-*X* silica, but this latter offered additional parameters that allowed us to adjust the pore size. The first example of a synthesis parameter-dependent pore size evolution was observed in our pristine one-step synthesis when changing the temperature of the reaction bath allowed us to obtain slight changes in the final pore size [11]. This was confirmed with the present two-step process [15–17]. In the course of this latter, we observed that the amount of fluoride salt was an unexpected parameter that allowed us to reach a similar result [16]. Therefore we carried out a complete study on the influence of these parameters and their effect could be easily explained on the light of the hybrid micelle structure [23].

The influence of TMB is reported in Fig. 10. As the TMB:surf. ratio increases, the silica pore diameter grows without any change in the silica wall thickness. A 0.5 nm increasing of the pore diameter is observed for TMB:surf. molar ratio varying from 0 to 2, but the silica wall remains unchanged. However, this effect is limited by the solubility of TMB and a larger addition gives heterogeneous mixtures that can even lead to mesostructured cellular foams [25,26].

We verified that the influence of the synthesis temperature on the nanostructure, could be extended to all classes of MSU-*X* silica. Fig. 11 reports the evolution of the pore diameter observed for different types of MSU-1 or MSU-4 materials (the question of MSU-3 synthesized with P123 tribloc-copolymer will be addressed thereinafter) [23]. For both families, a linear

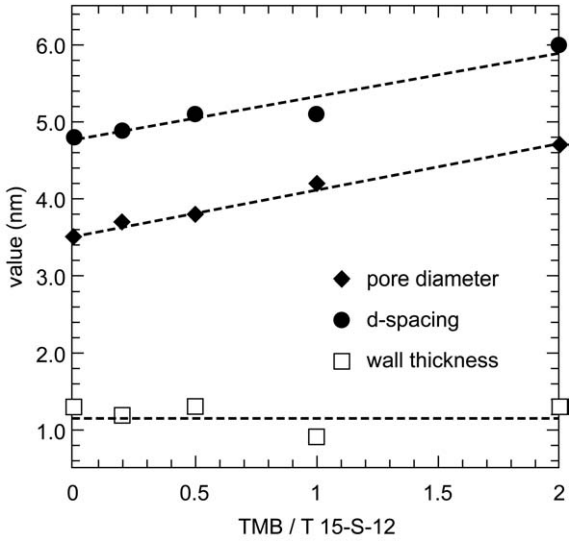

Fig. 10. Evolution of the *d*-spacing, pore diameter and wall thickness as a function of the TMB:surfactant molar ratio for calcined silica prepared with Tergitol 15-S-12. Dashed lines: linear fit of the evolution.

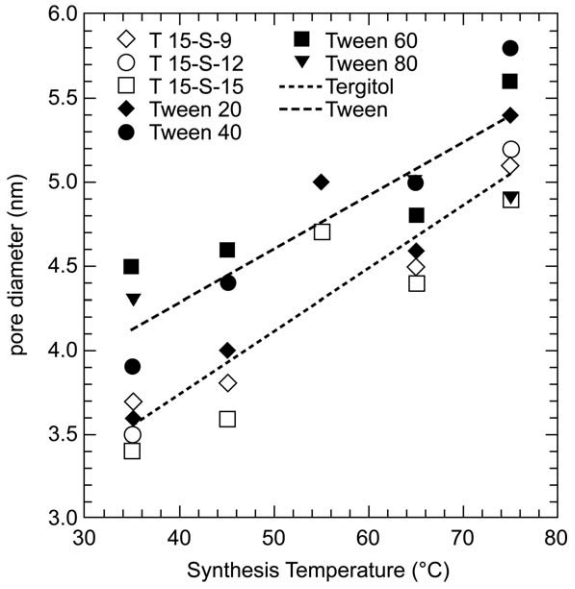

Fig. 11. Evolution as a function of the synthesis temperature of the pore diameter of MSU-1 and -4 silica prepared with different Tergitol 15-S-N and Tween templates. Dashed line: linear fit of the evolution, calculated with the whole set of samples of MSU-1 and MSU-4.

increase of 1.0 nm was observed for the pore diameter, when synthesis temperature varied between 35 and 75 °C. These observations confirmed that the pore size dependence as a function of the synthesis temperature, is a general feature of the two-step synthesis, whatever the surfactant.

The parallel study of *d*-spacing evolution (XRD) and pore diameter (N_2 adsorption isotherms) allowed us to establish that the silica wall thickness remains almost constant whatever the synthesis temperature. Thus, the synthesis temperature appears to be potentially a highly versatile parameter, and bigger pores could be expected. However, this effect is limited by the water boiling temperature, and the cloud point (CP) temperature of nonionic surfactants that makes the hydrophilic character to decrease with temperature. For instance, if CP is close to 100 °C for Tergitol 15-S-12 ($C_{15}(EO)_{12}$), the CP is only at 65 °C for the Tergitol 15-S-9 ($C_{15}(EO)_9$) and 35 °C for Tergitol 15-S-7 ($C_{15}(EO)_7$). Moreover, temperature speeds up the kinetics of silica condensation, which can prevent the formation of the hybrid micelles, prior to the formation of the silica framework (an increase of the concentration leads to the same result). This factor may lead to ill-ordered materials. Therefore the pore evolution can be controlled only in a certain range but this property belongs only to the syntheses based on nonionic templates and especially to the two-step process where the assembly mechanism is better controlled. This is a key factor for specific applications such as specialties chemistry or separation processes where an accurate control of pore size is required.

Surprisingly, a similar trend can be also obtained when sodium fluoride is added as catalyst, with a mean variation of 1.5 nm when $NaF:SiO_2$ varies between 0.5% and 6.0% (in mol; Fig. 12) [23]. The variation is not linear but it slows down as the amount of fluoride increases toward a limit. The combined influence of both parameters (temperature and catalyst) was verified (Fig. 13). Both the N_2 isotherms and the pore diameters calculated according to the Broekhoff and de Boer pore size distribution are reported [9].

It is clearly established that the combined variation of these parameters may allow us to tune the final porosity from less to 2.0–5.0 nm, with the same reacting medium. This pore control is achieved only because the hybrid micelles formed at the end of the assembly step are stable and dynamic. Fig. 14 displays an example of this adaptation: the size of nonionic micelles (circles) increases when the temperature increases. This behavior is reversible upon cooling down (see circle in a square). The same behavior is observed with the hybrid micelles (crosses). By taking into account this dynam-

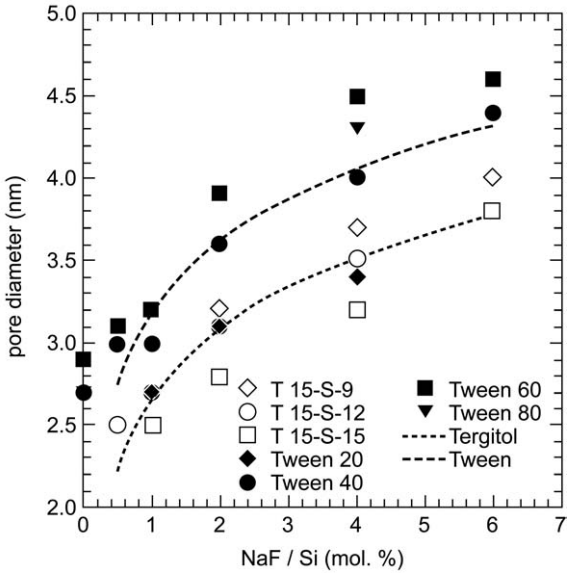

Fig. 12. Evolution as a function of the NaF/Si molar ratio of the pore diameter of MSU-1 and -4 silica prepared with different Tergitol 15-S-N and Tween templates. Dashed line: Log fit of the evolution of the parameters, calculated with the whole set of samples of MSU-1 and MSU-4.

ics, we were able to explain how changes in the environment of the hybrid micelles during reaction, could modify the final pore size of the mesoporous silica by shifting the boundary between the hydrophobic core and the hydrophilic shell that contains silica oligomers (Fig. 15) [23]. The simplest mechanism—which was widely used with all kind of syntheses—is provided by TMB that swells the alkyle core without disturbing the hydrophilic shell (Fig. 15B).

The future silica walls will be built from the micelle region that contains the diffuse silica framework and the future porosity will arise from the central zone that does not contain silica. Increasing the central hydrophobic region by dissolving TMB into it gives a material that exhibits larger pores with unchanged silica walls. However, this method can apply to relatively small amounts of TMB because its dissolution rate into the alkyle core is quite limited and leads quickly to microemulsions [26].

The pore size variation created by the temperature raising must be linked with the weakening of hydrogen bonding interactions that increases the hydrophobicity of PEO groups. This tends to expel more and more water molecules from this shell, to stretch the PEO chains and to increase the micelle size as it was reported in

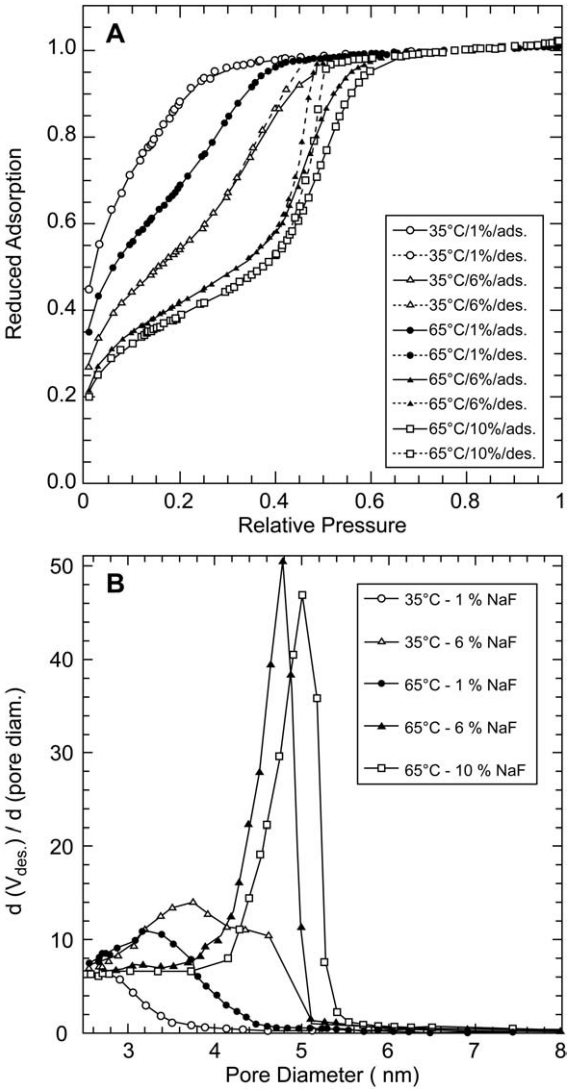

Fig. 13. (a) Normalized (at P/P_o = 0.98) nitrogen adsorption/desorption isotherms of MSU-1 silica prepared with Tergitol 15-S-12, at 35 or 65 °C and different NaF:Si molar ratios (1%, 6% and 10%) (b) pore size distribution deduced from the nitrogen desorption branch.

Fig. 15. The increasing hydrophobicity of the PEO groups will weaken the interactions with the silica oligomers, which will be pushed outside the micelle for entropic reasons and kept apart from the inner region of the hydrophilic shell. Finally, this internal part, freed from silica, will add to the hydrophobic core to contribute to the final porosity (Fig. 15C). In this case, temperature, which modifies the level of hydrophobicity of the PEO shell in the hybrid micelle, will shift the

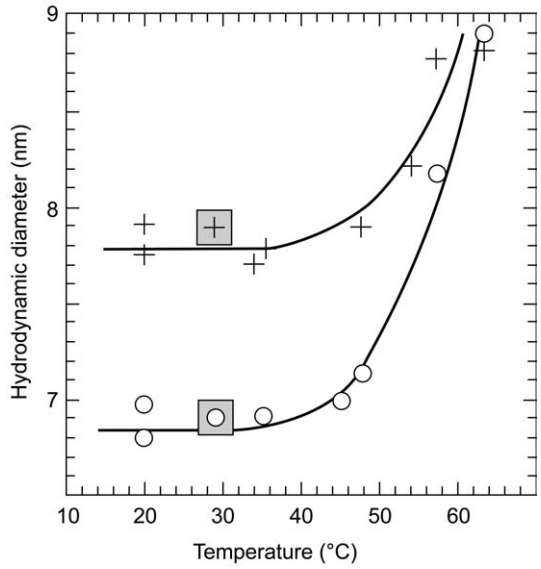

Fig. 14. Evolution of the hydrodynamic for (circles) pure micelles of Tergitol 15-S-12 and (crosses) hybrid micelles with TEOS:surf. =10, as a function of the temperature (calculated from DLS). square: size upon cooling.

frontier between the hydrophobic internal zone (internal core plus internal EO groups) free from silica and the external hydrophilic shell that contains EO groups, water and silica oligomers.

Even if it had been reported that fluoride salt may have an influence on the final structure of the mesoporous silica, our own experiences made with addition of large amounts of sodium chloride made us think that there is no 'salt effect' in this type of synthesis [16,17]. If a change in the ionic force of the solution does not modify the final structure, the influence of the sodium fluoride on the structure of MSU-*X* materials must be explained on the light of its catalytic properties that speed up the oxolation kinetics, leading to a progressive decrease of the amount of hydroxo groups linked to silica oligomers. This results in an increasing hydrophobicity of the silica framework—along with a decrease in its flexibility—that will expel it from the hydrophilic PEO shell. This will tend to shift outside the frontier between the outer hydrophilic PEO shell that contains silica and the inner hydrophilic PEO shell that does not contain it (Fig. 15D). In this case, the higher condensation of silica leads to a thinner thickness of the walls, which is actually observed [23]. One may summarize these results as follows: (i) TMB swells the hydrophobic core, (ii) temperature shifts the limit between the hydrophobic zone and the hydrophilic one, (iii) the catalyst limits the depth of penetration of silica into the hydrophilic shell. It appears that these three parameters do not act on the same part of the hybrid micelle, which explains why their effects are additive (Fig. 13). Finally, it is worth to note that sodium fluoride has also an effect on the particle size: increasing the NaF:Si ratio will increase the amount of silica seeds, which results in a general decreasing of the overall particle size (Fig. 16).

As pointed out previously, MSU-type mesoporous silica prepared with nonionic surfactants according to the two-step pathway, exhibits a specific feature that makes its structure sensitive to the synthesis temperature. Usually, this factor modifies the pore structure in the mesoporous range, between 2 and 5 nm. Nevertheless, when Pluronic P123 ($(PEO)_{20}(PPO)_{70}(PEO)_{20}$) is used, the pore size can vary from microporous (below 2 nm) created by the trapping of single molecules in the silica network, to mesoporous (close to 9 nm) in a steady-like evolution (Fig. 17) [27]. This feature was explained by the specific properties of block copolymers that form no micelles below a critical micelle temperature (CMT) due to the relative hydrophilicity of the PPO chains. This is combined with phase separation above the CP at higher temperature, due to the increasing hydrophobicity of the PEO chains.

5. The shape control

Most of the preparations based on this two-step pathway gave micrometric spherical particles. However, different parameters allowed us to obtain more specific morphologies, among them being the formation of perfectly hexagonal structures obtained with Tween 60 and Pluronic P123 bloc-copolymer, which will be described in the following. Original morphologies were obtained by playing with the hydrophobic character of TEOS when it is dispersed in an aqueous solution of surfactant. In the normal two-step process, the synthesis of MSU-*X* silica is made at pH 2–4, when TEOS is hydrolyzed into the hybrid micelles, prior to the silica condensation step. Under neutral pH conditions, TEOS cannot be hydrolyzed readily and it remains as a hydrophobic oil whose dilution into the aqueous solution of surfactant must be helped by energetic stirring such as ultrasound. One obtains a complex emulsion whose the

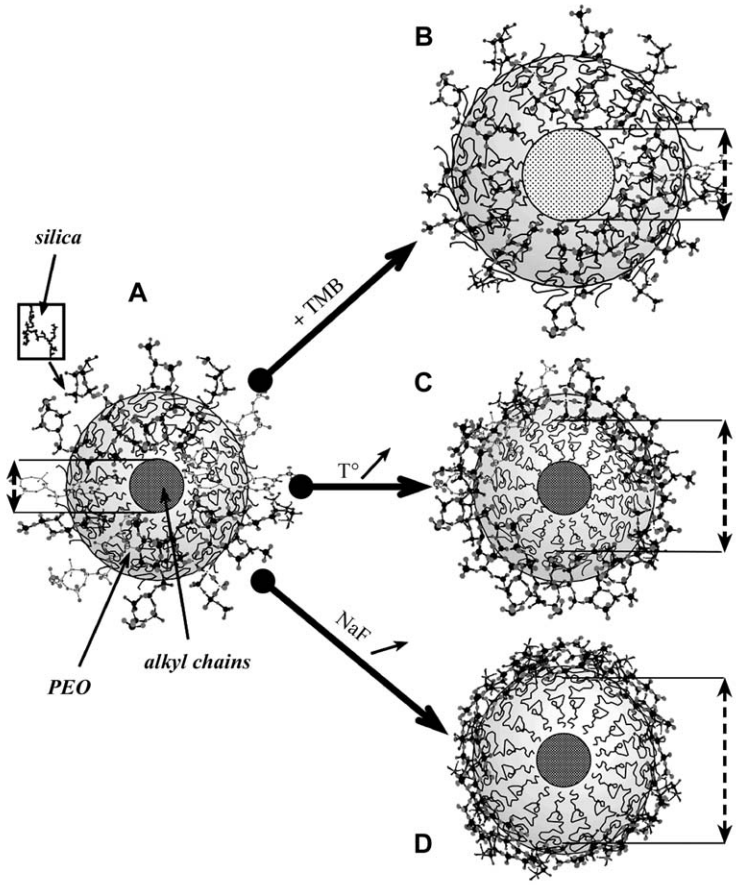

Fig. 15. Scheme of the influence of the different parameters on the hybrid micelle structure: (**A**) initial structure, (**B**) the addition of TMB swells the alkyl core, (**C**) increasing temperature increases the hydrophobicity of PEO chains, (**D**) increasing the NaF:Si ratio increases the hydrophobicity of silica. Dashed double arrows: new silica-free core diameter precursor of the porosity.

level of intimacy – depending on the strength of sonication – will define the final structure of the silica framework [28].

When the sonication is correctly adjusted, the cavitation bubbles can be trapped by this emulsion and template future voids in the inorganic framework. The final structure will hence depend on the degree of intimacy between hydrophilic and hydrophobic components and gas bubbles. When sonication is tuned above an effective power of 40 W (120-W assigned power), the nanostructure of the material is preserved but the silica framework is structured around the cavitation bubbles, which leads to hollow particles with mesoporous walls (Fig. 18) that exhibit a huge N_2 adsorption/desorption isotherm loop [28,29]. Moreover, increasing the overall concentration and still applying a strong sonication may lead to a similar phenomenon at a higher level where eggshell-like particles are obtained (Fig. 19) [30].

Syntheses performed with relatively hydrophobic templates such as Pluronic P123 bloc-copolymer or sorbitan ester Tween 60, gave different results. We observed that a fine control of the synthesis parameters (concentration, pH, temperature) could lead to hexagonal framework [16,27]. In the case of P123, stick-like particles were obtained with a perfect hexagonal stacking of parallel pores (Fig. 20).

Changing slightly the synthesis parameters but still using Pluronic P123, allowed us to prepare of a new type of mesoporous silica made of nanoparticles (200 nm in size) built by the folding of ribbons with a hexagonal porosity (pore diameter of 8.6 nm). This folding created an additional porosity by the formation

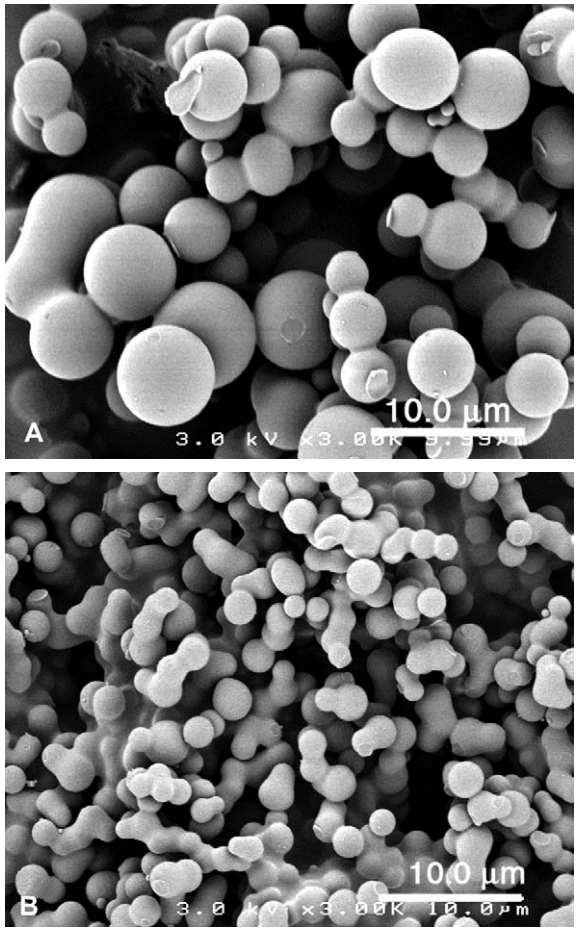

Fig. 16. SEM observation of calcined mesoporous silica prepared at 65 °C with (**A**) a Si:surf. ratio of 1 mol% and (**B**) a Si:surf. ratio of 10 mol%.

microvoids inside the particles (Fig. 21). Their structure was especially illustrated by TEM 3D rebuilding tomography [31].

6. Liquid filtration

Membranes are semipermeable barriers that prevent two phases from getting into contact. This barrier must be permselective, that is, it must allow only some components of one phase to diffuse into the other. Therefore the transport properties of membranes depend highly on the membrane microstructure, including pore shape and morphology, pore size distribution and tortuosity. Inorganic membranes are usually designed for tangential liquid filtration were a primary liquid or suspension flows into a cylindrical porous tube made of the membrane supported onto a porous ceramic substrate. The filtration force is governed by a pressure applied across the tube. Since the membrane itself must

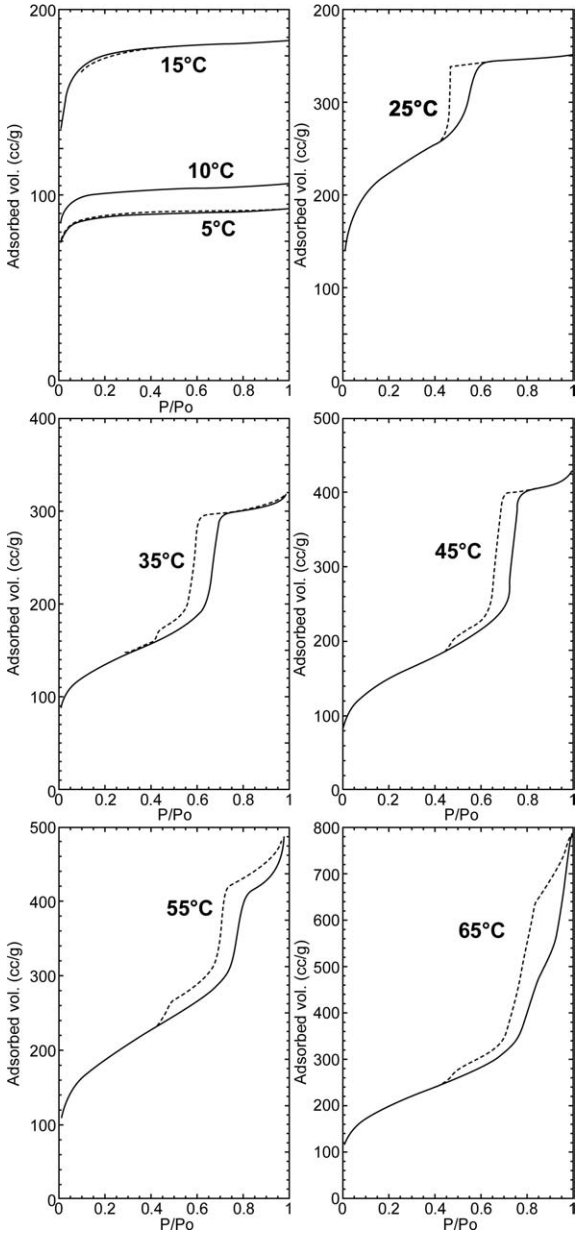

Fig. 17. Nitrogen adsorption/desorption isotherms of calcined MSU-3 silica prepared at different temperatures ranging between 5 and 65 °C. As the synthesis temperature increases, the adsorption edge shifts from microporosity to well-defined structural mesoporosity, then ill-defined textural mesoporosity.

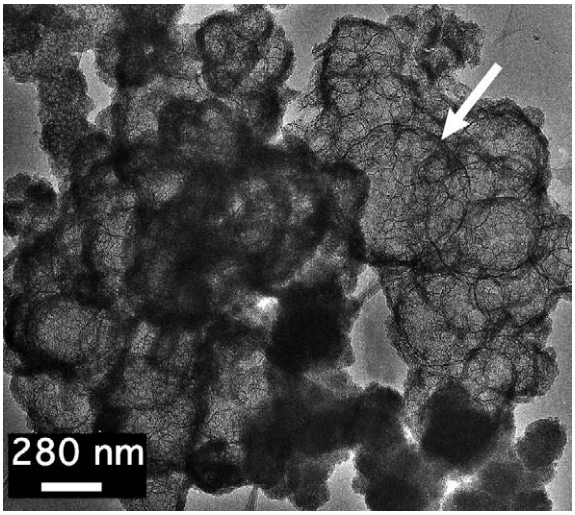

Fig. 18. TEM analysis of calcined silica prepared with a 120 W assigned sonication power.

be as thin as possible to prevent a decrease of the diffusion flow below unacceptable values, it is always deposited onto one or several stacked macroporous layers that provide the mechanical strength required for easy handling. Except the size exclusion mechanism observed with any kind of membrane, filtration mechanisms working for low ultrafiltration (UF) and nanofiltration (NF) membranes, are also based on electrostatic repulsion between the superficial charge of the membrane and solubilized species. Preparation of NF and UF inorganic membranes usually involves the deposition of a thin layer of colloidal particles that is subsequently partially densified (sintered) by an adequate thermal treatment. The final porosity of the membrane is controlled by the size of the pristine colloidal particles that defines the final interparticle voids after sintering. In this case, particles themselves are dense and porosity of the filtration layer is provided by the inter-

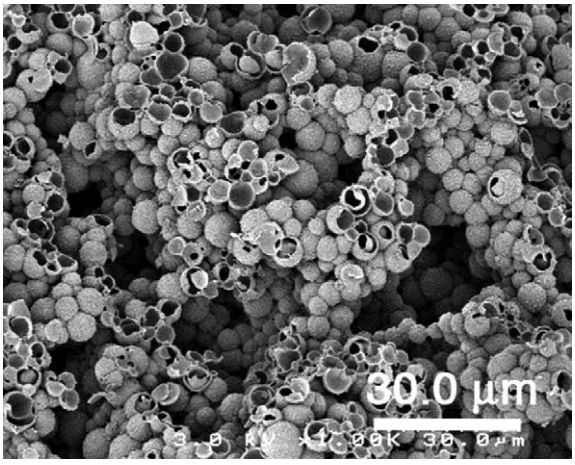

Fig. 19. SEM analysis of eggshell calcined particles obtained after strong sonication with a Si:surf. ratio of 8 and a 0.4 mol l^{-1} concentration of Tergitol 15-S-12.

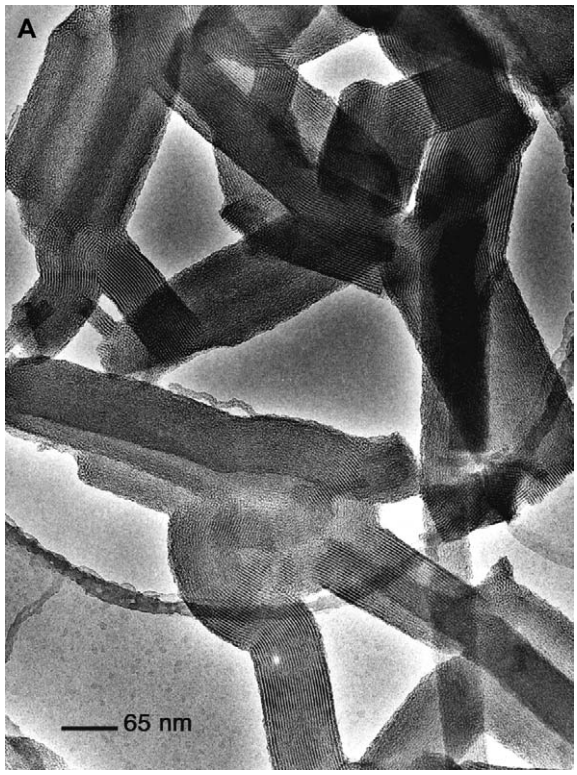

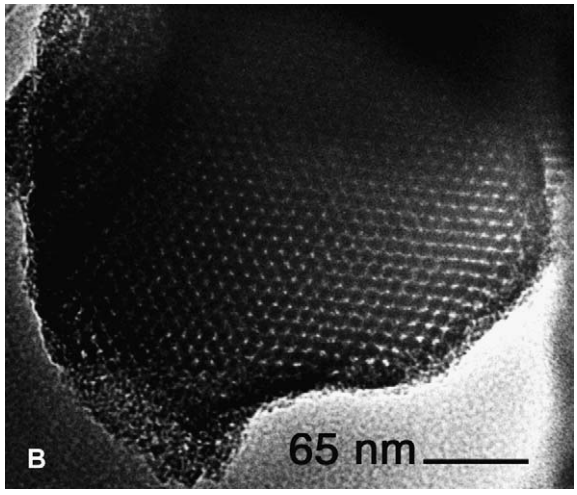

Fig. 20. TEM observation of calcined stick-like MSU-3 silica prepared with Pluronic P123 copolymer.

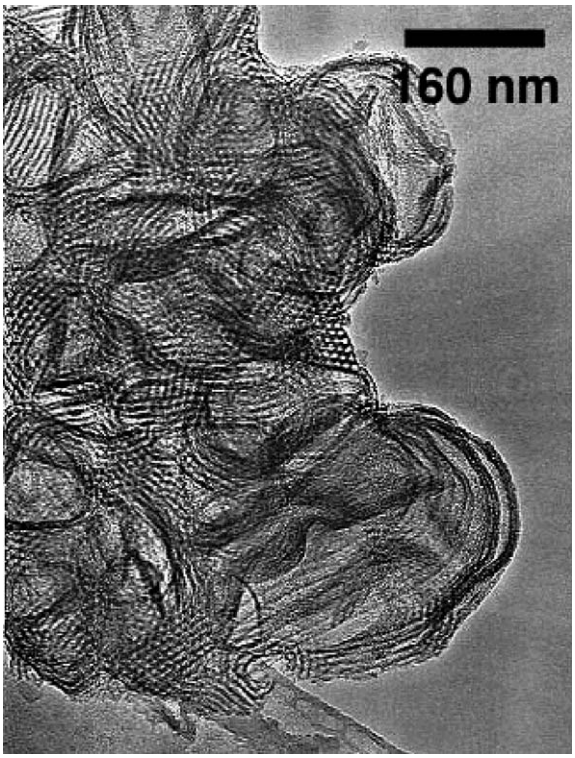

Fig. 21. TEM observation of calcined ribbon-like MSU-3 silica prepared with Pluronic P123 copolymer.

particle (textural) porosity. Membranes were also prepared with materials such as zeolites, which exhibit an intrinsic porosity [32–34]. The expectations were to obtain membranes with a very well-defined pore size. In that case, synthesis is much more difficult because the achievement of a membrane based on a defect-free continuous layer is required instead of a stacking of single porous particles. Hence, we adapted our synthesis for the preparation of a membrane dedicated to liquid filtration. Since the two-step reaction includes the formation of hybrid micelles that will be further destabilized by the addition of sodium fluoride, we were able to direct the reaction onto the surface of the porous substrate impregnated with a solution of sodium fluoride thanks to an interfacial reaction (Fig. 22). The membrane is thus localized at the interface between the surface of the ceramic porous substrate and the solution of hybrid micelles and the silica layer grows at the encountering surface onto the porous support [35,36].

The rejection efficiency of the membrane was tested in water as a function of the acidity, with hydrophilic PEO polymers of molecular weights ranging from 600 to 10,000. The rejection rate is reported in Fig. 23. Obviously, the general behavior cannot be described as a simple steric rejection mechanism. First, as expected, one observes for neutral pH a steep increasing of the rejection rate, between PEO 600 and the PEO 10,000.

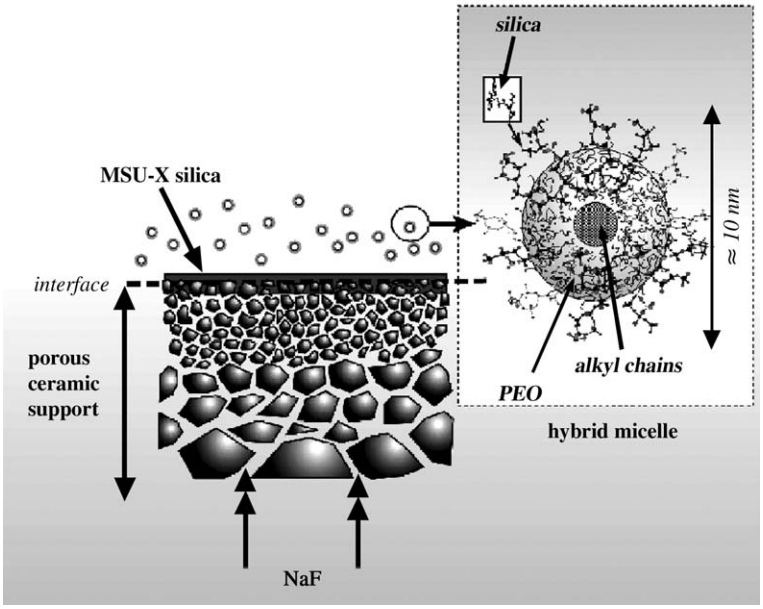

Fig. 22. Scheme of the interfacial reaction leading to a mesoporous silica membrane from a solution of hybrid micelles.

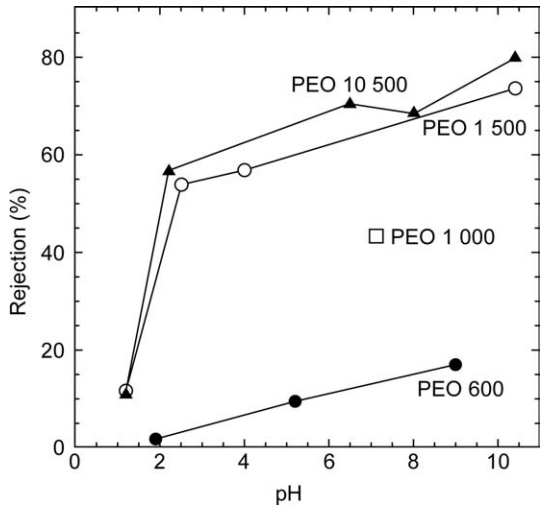

Fig. 23. Evolution of the rejection rate of the silica mesoporous membrane as a function of the pH, for different polymers. At pH 7, the cut-off of the silica membrane can be assigned between PEO 1000 and PEO 1500 corresponding to a pore diameter of 2.5 nm. The test was performed in water with filtration pressure ΔP set at 4 bar.

This confirms that the silica layer exhibits a narrow pore size distribution with a cut-off at Y 2000 Da, corresponding to a pore diameter lying between 2.0 and 3.0 nm. As pH decreases from 10 to 2, only a slight decrease in the rejection rate is observed, but below pH 2, one observes a total loss of retention, even for PEO 10,000 that exhibits a mean hydrodynamic diameter of 6.8 nm, that is, two to three times the pore diameter. The origin of this unusual behavior was explained by two arguments, one regarding the chemical nature of the membrane and its influence on electrostatic repulsions, the other taking into account the cylindrical shape of sparely connected pores, as revealed by TEM observations that showed an unexpected parallel alignment of 30 nm thick mesoporous silica domains, the pores being oriented almost orthogonally to the support surface [35]. This structure was explained by the columnar growth of silica building blocks, induced by the diffusion of fluoride ions out of the support pores.

Our interpretation regarding the filtration properties was based on works reported by Zitha and de Gennes groups [36–39]. PEO polymer chains in solution behave like statistical spherical coils whose shape is a result of an equilibrium between the trend of EO groups to stretch and the entropic string effect that makes them shrink. This equilibrium can be disrupted if an external parameter is introduced, such as specific interactions between PEO and the silica surface inside the pores. Since the PEO oxygen atoms bear a significant negative charge, they will interact attractively or repulsively with the silica whose surface charge will depend on the medium acidity. Above pH 2, that is, above the silica iso-electric point (IEP), neutral silica will not ease the interaction with the PEO oxygen atoms and the rejection cut-off will thus depend only on a size exclusion. Below pH 2, positively charged silica will provide an additional strain term that will allow the polymer to stretch enough to enter the pore. The liquid flow will then allow it to slide into the pore. Of course, this argument can work only if the polymers do not block across pore necks formed between particles, which would finally lead quickly to the commonly observed membrane fouling. This bridging mechanism described by Zitha et al. [39], explains perfectly the fouling mechanism in granular membranes, but it cannot apply to ours since it presents non-connecting parallel pores [36]. The polymer will thus be confined within the cylindrical pore and will be pushed throughout by the flow pressure.

7. HPLC chromatography

Among the possible applications for mesoporous silica, HPLC separation affords good potential because it requires a rather small amount of material for a high value application. This application was studied by different groups, since several years [40–45]. The two-step synthesis of MSU-*X* silica was also tuned in order to fulfill some of the requirements needed to obtain a correct column packing, including a narrow particle size distribution in the micrometric range and correct particles stacking. We were able to achieve this process by simple techniques and we demonstrated that ungrafted mesoporous silica prepared according to our pathway, could lead to separations comparable with those obtained with commercial powders (Nucleosil 50-7 from Macherey Nagel Co.) [46,47]. The result displayed in Fig. 24a, confirms that the separation of four different components (benzene, diphenyle, naphthalene, phenantrene) in hexane is effective with a 20 cm length column.

However, the higher surface area of the MSU mesoporous silica (800 $m^2\ g^{-1}$ to be compared with 250 $m^2\ g^{-1}$ for the commercial powder) led to longer

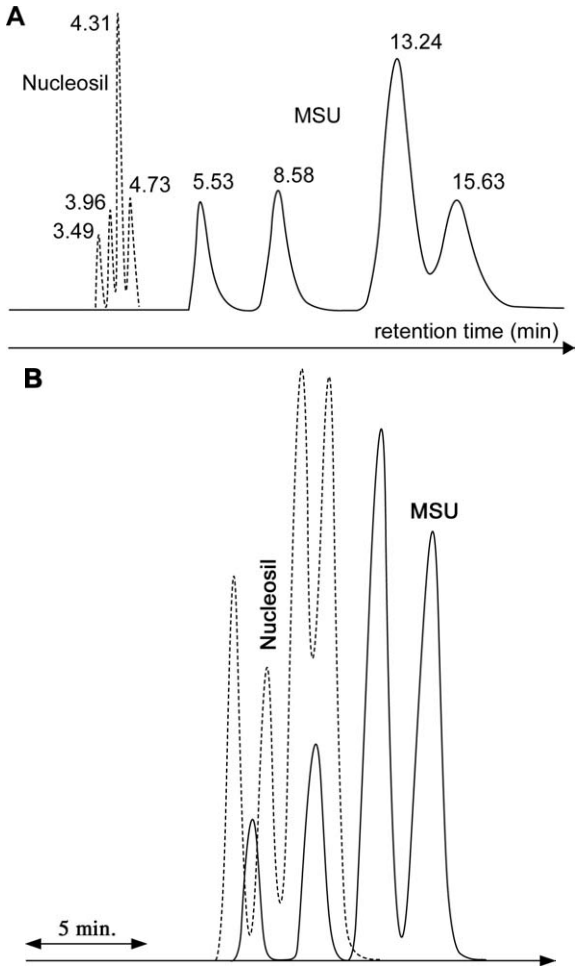

Fig. 24. Retention time of a mixture of benzene (first peak), diphenyle (second peak), naphtalene (third peak) and phenantrene (fourth peak) for ungrafted powders. eluents: (**A**) in cyclohexane for both columns; (**B**) in cyclohexanefor the commercial and in a 20:80 dichloroethane:cychlohexane solution for our powder.

retention times that gave the peak wings on the right side of each. Since the separation mechanism, in this case, is based on preferential adsorption, we could adjust the competitive adsorption between molecules and solvent by increasing the polarity of this latter by the addition of dichloromethane. In that case, the retention times between the two columns were equivalent and the column filled with MSU silica was still efficient (Fig. 24b).

Finally, we demonstrated also that a new approach based on the use of the ribbon-like submicronic powders could work, even if they were supposed to be too small for this application (Fig. 21) [31]. Their large surface area combined with their specific shape and hierarchical porosity allowed us to prepared efficient ungrafted short columns (6 cm length) that could separate mixtures of organic solvents (Fig. 25).

8. Conclusion

There have been thousand of syntheses of mesoporous silica within the 10 last years. Among them, some processes, which would appear as similar, led surprisingly to totally different materials or were hardly reproducible. This could be explained easily once one bears in mind the drastic influence that some slight changes in the synthesis parameters (concentration, temperature, precursors, pH...) may have on both the thermodynamic and kinetic properties. This means also that it is quite difficult to compare different types of syntheses even if they used the same templating agents, as far as the conditions were not close. Indeed, the control of the two main steps, namely the assembly of silica with templates and the silica condensation that freezes this assembly, are the key factor for achieving successful and reproducible syntheses. We developed a specific pathway, based on the use of nonionic surfactant. Even if the two-step synthesis of MSU silica was not explored as widely as that of MCM-41 or SBA-15 materials, it offers nevertheless some unique properties that should be developed in the future. For instance, the templates are rather inexpensive and environment-friendly, the synthesis proceeds at room temperature and ambient pressure with a very good control over it. Moreover, unlike syntheses of MCM or SBA-type mesoporous silica that use only a small range of templates (cetyltrimethylammonium, Pluronic P123), the two-step synthesis of MSU-type silica can apply usefully to a wide range of surfactants or copolymers, and it gives high yields with good reproducibility, whatever the reactor volume. Moreover, the intermediate formation of stable hybrid micelles is unique and provides a very good control over the kinetics that may help to tune the final product for specific applications such as those in separation processes that were described in the present review.

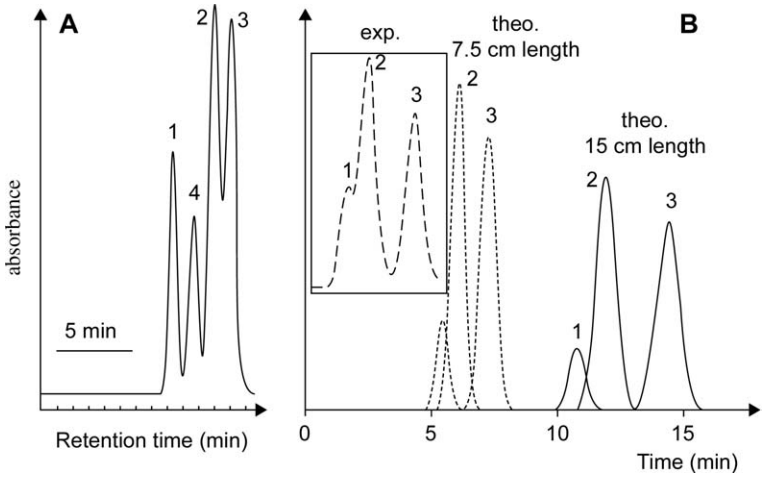

Fig. 25. HPLC separation tests performed with benzene (**1**), naphthalene (**2**), phenantrene (**3**) and biphenyl (**4**) for: (**A**) a commercial powder with a column length of 25 cm; (**B**) the ribbon-like MSU-3 powder with a column length of 6 cm along with theoretical chromatograms calculated for different lengths.

References

[1] F. Di Renzo, H. Cambon, R. Dutartre, Microporous Mater. 10 (1997) 283.
[2] C.T. Kresge, M.E. Leonowicz, W.J. Roth, J.C. Vartuli, J.S. Beck, Nature 359 (1992) 710.
[3] J.S. Beck, J.C. Vartuli, W.J. Roth, M.E. Leonowicz, C.T. Kresge, K.D. Schmitt, C.T.-W. Chu, D.H. Olson, E.W. Sheppard, S.B. McCullen, J.B. Higgins, J.L. Schlenker, J. Am. Chem. Soc. 114 (1992) 10834.
[4] S. Inagaki, Y. Fukushima, K. Kuroda, J. Chem. Soc., Chem. Commun. (1993) 680.
[5] S. Inagaki, A. Koiwai, N. Suzuki, Y. Fukushima, K. Kuroda, Bull. Chem. Soc. Jpn 69 (1996) 1449.
[6] P. Tanev, T.M. Chibwe, T.J. Pinnavaia, Nature 368 (1994) 321.
[7] P. Tanev, T.T.J. Pinnavaia, Science 267 (1995) 865.
[8] S.A. Bagshaw, É. Prouzet, T.J. Pinnavaia, Science 269 (1995) 1242.
[9] É. Prouzet, F. Cot, G. Nabias, A. Larbot, P.J. Kooyman, T.J. Pinnavaia, Chem. Mater. 11 (1999) 1498.
[10] A.C. Voegtlin, F. Ruch, J.L. Guth, J. Patarin, L. Huve, Microporous Mater. 9 (1997) 97.
[11] É. Prouzet, T.J. Pinnavaia, Angew. Chem. Int. Ed. Engl. 36 (1997) 516.
[12] D. Zhao, J. Feng, Q. Huo, N. Melosh, G.H. Fredrickson, B.F. Chmelka, G.D. Stucky, Science 279 (1998) 548.
[13] D. Zhao, Q. Huo, J. Feng, B.F. Chmelka, G.D. Stucky, J. Am. Chem. Soc. 120 (1998) 6024.
[14] J.L. Blin, A. Léonard, B.L. Su, Chem. Mater. 13 (2001) 3542.
[15] C. Boissière, A. Van der Lee, A. El Mansouri, A. Larbot, É. Prouzet, J. Chem. Soc. Chem. Commun. 20 (1999) 2047.
[16] C. Boissière, A. Larbot, A. Van der Lee, P.J. Kooyman, É. Prouzet, Chem. Mater. 12 (2000) 2902.
[17] C. Boissière, A. Larbot, É. Prouzet, Chem. Mater. 12 (2000) 1937.
[18] C.J. Brinker, J. Non-Cryst. Solids 100 (1988) 31.
[19] C.J. Brinker, J. Collins, C.-Y. Tsai, Y. Lu, DOE report 97MC28074.
[20] Y. Liu, W. Zhang, T.J. Pinnavaia, Angew. Chem. Int. Ed. Engl. 40 (2001) 1255.
[21] T. Zemb, Colloids Surf. A 435 (1997) 129–130.
[22] T. Zemb, in: P. Lindner, T. Zemb (Eds.), Neutrons, X-rays and Light, Elsevier, 2002.
[23] C. Boissière, M.A.U. Martines, M. Tokomuto, A. Larbot, É. Prouzet, Chem. Mater. 15 (2003) 509.
[24] C. Boissière, A. Larbot, C. Bourgaux, É. Prouzet, C.A. Bunton, Chem. Mater. 13 (2001) 3580.
[25] P. Schmidt-Winkel, W.W.J. Lukens, P. Yang, D.I. Margolese, J.S. Lettow, J.Y. Ying, G.D. Stucky, Chem. Mater. 12 (2000) 686.
[26] P. Schmidt-Winkel, C.J. Glinka, G.D. Stucky, Langmuir 16 (2000) 356.
[27] M.A.U. Martines, E. Yeong, A. Larbot, É. Prouzet, Microporous Mesoporous Mater. 74 (2004) 213.
[28] F. Cot, P.J. Kooyman, A. Larbot, É. Prouzet, in: L. Bonneviot, F. Beland, C. Danumah, S. Giasson, S. Kaliaguine (Eds.), Mesoporous Molecular Sieves, 117, Elsiever, Amsterdam, Lausanne, New York, Oxford, Shannon, Singapore, Tokyo, 1998, p. 231.
[29] É. Prouzet, F. Cot, C. Boissière, P.J. Kooyman, A. Larbot, J. Mater. Chem. 12 (2002) 1553.
[30] É. Prouzet, unpublished results.
[31] M.A.U. Martines, E. Yeong, M. Persin, A. Larbot, W.F. Voorhout, C.K.U. Kübel, P.J. Kooyman, É. Prouzet, C.R. Chimie 8 (2005).
[32] K.C. Jansen, E.N. Coker, Curr. Opin. Solid-State Mater. Sci. 1 (1996) 65.
[33] T.R. Gaffney, Curr. Opin. Solid-State Mater. Sci. 1 (1996) 69.
[34] Z. Lai, G. Bonilla, I. Diaz, G. Nery, K. Sujaoti, M.A. Amat, E. Kokkoli, O. Terasaki, R.W. Thompson, M. Tsapatsis, D.G. Vlachos, Science 300 (2003) 456.

[35] C. Boissière, M.A.U. Martines, P.J. Kooyman, T.R. de Kruijff, A. Larbot, É. Prouzet, Chem. Mater. 15 (2003) 460.
[36] C. Boissière, M.A.U. Martines, A. Larbot, É. Prouzet, J. Membr. Sci. (in press)
[37] C. Gay, P.-G. de Gennes, E. Raphaël, F. Brochard-Wyart, Macromolecules 29 (1996) 8379.
[38] P.-G. de Gennes, Adv. Polym. Sci. 138 (1999) 91.
[39] P.L.J. Zitha, G. Chauveteau, L. Leger, J. Colloids Interf. Sci. 234 (2001) 269.
[40] K.W. Gallis, A.G. Eklund, S.T. Jull, J.T. Araujo, J.G. Moore, C.C. Landry, in: A. Sayari, M. Jaroniec, T.J. Pinnavaia (Eds.), Nanoporous Materials II, Vol. 129, Elsevier, 2000.
[41] T. Nassivera, A.G. Eklund, C.C. Landry, J. Chromatogr. A. 973 (2002) 97.
[42] Y. Ma, L. Qi, J. Ma, Y. Wu, O. Liu, H. Cheng, Colloids Surf. A 229 (2003) 1.
[43] M. Mesa, L. Sierra, B. Lopez, A. Ramirez, J.-L. Guth, Solid-State Sci. 5 (2003) 1303.
[44] T. Shindo, H. Kudo, S. Kitabayashi, S. Ozawa, Microporous Mesoporous Mater. 63 (2003) 97.
[45] A.L. Doadrio, E.M.B. Sousa, J.C. Doadrio, J. Perez Pariente, I. Izquierdo-Barba, M. Vallet-Regi, J. Control. Release 97 (2004) 125.
[46] C. Boissière, A. Larbot, É. Prouzet, in: A. Sayari, M. Jaroniec, T.J. Pinnavaia (Eds.), Nanoporous Materials II, 129, Elsevier, Banff, Alberta, Canada, 2000, p. 31.
[47] C. Boissière, M. Kümmel, M. Persin, A. Larbot, É. Prouzet, Adv. Funct. Mater. 11 (2001) 129.